MHD Pulsatile Flow of a Conducting Fluid Sandwiched Between Viscous Fluids Inside Permeable Beds

Deepak Kumar[1*] **and Manju Agarwal**[2]

[1]*Department of Mathematics and Astronomy, University of Lucknow, Lucknow, India, Pin-226007*
[2]*Departmet of Mathematics and Astronomy, University of Lucknow, Lucknow, India, Pin-226007*
[*]*Corresponding author E-mail: deepakpatel0412@gmail.com*

Abstract

In the present paper the problem of MHD pulsatile flow of a viscous conducting fluid in porous medium sandwiched between viscous fluids is investigated inside permeable beds. The flow in porous region is modelled using Brinkman equation and in the permeable beds by Darcy's law. The Beavers Joseph slip boundary condition is used at the interfaces of permeable beds. The governing partial differential equations of flow are transformed in to ordinary differential equations by separating steady and oscillatory terms. The differential equations are solved analytically and the expressions for velocity, mass flux and shear stress are obtained. The analytical solutions are evaluated numerically and depicted graphically to show the effects of physical governing parameters on velocity and shear stress.

Keywords: Beavers-Joseph slip boundary condition, Brinkman equation, Immiscible fluids, Permeable beds, Pulsatile flow.
2010 Mathematics Subject Classification: 76S99; 76T99.

1. Introduction

From many decades the analysis of multiphase flow in porous media and inside permeable beds is in principal interest of scientists and engineers because of its numerous applications in natural systems like ground water flows, biomechanics, drainage, rain, blood flow inside an artery etc. as well as in many engineering problems like power generation, distillation of water, refrigeration etc. One of the major application of study of multiphase flow is in petroleum industry where flow of many immiscible fluids occur in the reservoir rock of oil field. A special kind of unsteady flow in which a periodic variation in flow velocity is superimposed on steady flow velocity is pulsatile flow and occurs in natural systems like cardiovascular systems in human respiratory[8], blood flow in arteries[11] etc. Carpinlioglu[3] presented a complete overview on pulsatile flow in his review article.

Governing equations of fluid motion in porous media and boundary conditions at different interfaces are reviewed by D.A.Nield [4]. M. Zamir[20] elaborated fluid dynamics of steady and pulsating flow and its applications. P. Bhattacharyya[2] studied laminar flow in a channel, considering that one boundary wall is porous and obtained analytical results by implementing B-J slip condition at porous wall. After that Venugopal and Bathaiah[18] analysed MHD Couette, Poiseuille and surface flows over a permeable bed. Unsteady oscillatory flow and heat transfer in composite porous medium is studied by Umavathi et.al.[16]. Iyengar and Bitla[5] reported expressions of velocity and mass flux for an incompressible couple stress fluid between permeable beds. Flow inside a permeable bed under exponentially decaying pressure gradient is investigated by Prasad and Kumar[10]. Jogie and Bhatt[6] studied flow of immiscible fluids in a naturally permeable channel using B-J slip condition. After that Sreenadh et.al.[13] analysed two phase flow between permeable beds by taking one couple stress fluid and the other Newtonian fluid. P. Sulochaana[15] reported MHD flow of couple stress fluid with periodic body acceleration. She reported that when body acceleration dominates pulsation pressure gradient, body acceleration promotes flow while body acceleration supress flow when pulsation gradient dominates body acceleration. Recently Khan and Zaman[7] obtained analytical expressions for velocity and shear stress of an unsteady MHD flow of second grade fluid, generated by accelerating plate. Flow of second grade fluid through constricted tube is discussed by Siddiqui et.al.[12]. Srinivas and Murthy[14] studied flow of two immiscible couple stress fluids between permeable beds and concluded that presence of couple stress decrease flow velocity. Three layer fluid flow over a small obstruction on the bottom of a channel is studied by S. Panda et.al.[9].Umavathi et.al.[17] studied unsteady flow in porous medium sandwiched between viscous fluids.

In view of various applications of flow in permeable beds, MHD flow and pulsatile flow in natural and human systems, we analyse flow of a conducting fluid in porous medium sandwiched between two viscous fluids inside permeable beds. We follow the momentum equation [19] for flow through porous media including fluid inertia and viscous stress in addition to Darcy's law.

$$\rho\{\frac{\partial V}{\partial t}+(\nabla.V)\nabla\} = -\nabla P+\mu\nabla^2 V-\frac{\mu}{K}V,$$
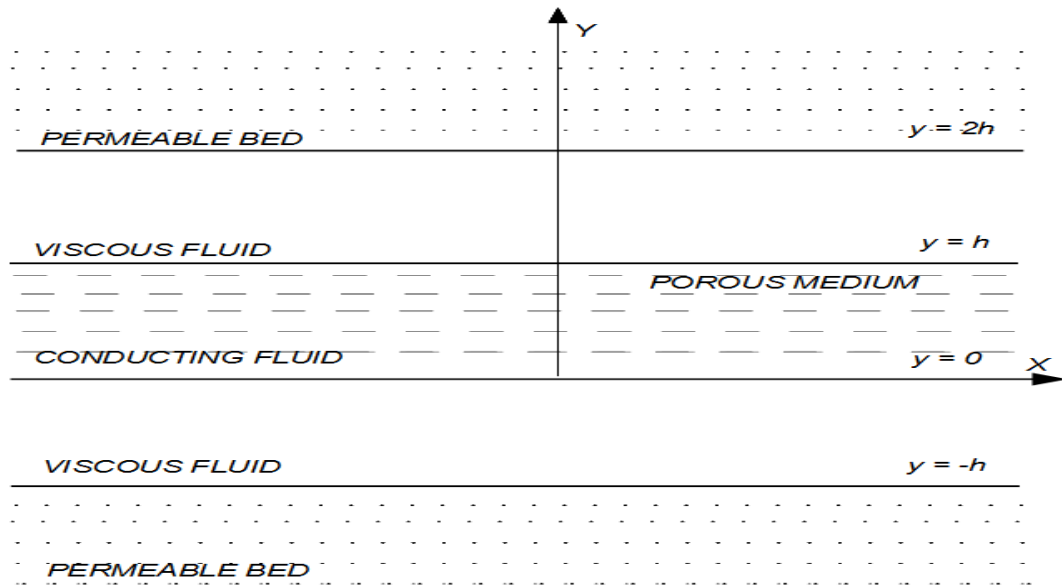
Figure 2.1

where

ρ is the fluid density

μ is the coefficient of viscosity

P is the pressure

V is the fluid velocity vector

K is the permeability of the porous medium

We use matching conditions (continuity of velocity and shear stress) at the interfaces but at the permeable beds we use the Beavers and Joseph[1] slip boundary condition

$$\frac{\partial u_f}{\partial y} = \frac{\alpha}{K^{\frac{1}{2}}} (u_f - u_m).$$

Here the clear fluid region occupies the region ($y > 0$), u_f is the fluid velocity and u_f and $\frac{\partial u_f}{\partial y}$ are evaluated at $y = 0+$. The Darcy velocity u_m is evaluated at some small distance from $y = 0$ in the porous medium. The Beaver-joseph constant α is dimensionless constant, depends on structure of porous medium and independent of the fluid viscosity.

2. Mathematical Formulation

The geometry under consideration is illustrated in Fig. 2.1, consists of a region inside permeable bed. The region-II ($0 \le y \le h$) is occupied by a conducting fluid of density ρ_2, viscosity μ_2 , the region-I ($-h \le y \le 0$) is filled with a viscous fluid of density ρ_1 and viscosity μ_1. Region-III ($h \le y \le 2h$) is also filled by a viscous fluid of density ρ_3 and viscosity μ_3. Here $\rho_1 > \rho_2 > \rho_3$.

We consider the permeable beds to be homogeneous and the fluids to be incompressible and immiscible. The flow is unsteady, laminar and fully developed and driven only by a pulsatile pressure gradient

$$-\frac{\partial p}{\partial x} = \left(\frac{\partial p}{\partial x}\right)_s + \left(\frac{\partial p}{\partial x}\right)_o e^{i\omega t},$$

where $\left(\frac{\partial p}{\partial x}\right)_s$ and $\left(\frac{\partial p}{\partial x}\right)_o$ are amplitudes of steady and oscillatory pulsations respectively and w is the frequency. It is noted that the viscous fluids and conducting fluid are immiscible (that is there exist no mixing between the fluids) and the constitutive equations for viscous fluids and conducting fluid are different.

Assuming that non zero component of velocity is X-component(that is the flow is one dimensional), the governing equations of fluid flow are

Region-I   Equation of mass balance

$$\frac{\partial u_1}{\partial x} = 0. \tag{2.1}$$

Equation of momentum balance

$$\rho_1 \frac{\partial u_1}{\partial t} = -\frac{\partial p}{\partial x} + \mu_1 \frac{\partial^2 u_1}{\partial y^2}. \tag{2.2}$$

Region-II   Equation of mass balance

$$\frac{\partial u_2}{\partial x} = 0. \tag{2.3}$$

Equation of momentum balance

$$\rho_2 \frac{\partial u_2}{\partial t} = -\frac{\partial p}{\partial x} + \mu_2 \frac{\partial^2 u_2}{\partial y^2} - \frac{\mu_2}{K_2} u_2 - \sigma B_o^2 u_2.$$

(2.4)

Region-III   Equation of mass balance

$$\frac{\partial u_3}{\partial x} = 0.$$

(2.5)

Equation of momentum balance

$$\rho_3 \frac{\partial u_3}{\partial t} = -\frac{\partial p}{\partial x} + \mu_3 \frac{\partial^2 u_3}{\partial y^2}.$$

(2.6)

Herein the velocities $u_1(y,t), u_2(y,t), u_3(y,t)$ are to satisfy the conditions

$$
\begin{aligned}
\frac{\partial u_1}{\partial y} &= \frac{\alpha}{\sqrt{K_1}}(u_1' - Q_1) && \text{at } y = -h, \\
u_1' &= u_1 && \text{at } y = -h, \\
\mu_1 \frac{\partial u_1}{\partial y} &= \mu_2 \frac{\partial u_2}{\partial y} && \text{at } y = 0, \\
u_1 &= u_2 && \text{at } y = 0, \\
\mu_2 \frac{\partial u_2}{\partial y} &= \mu_3 \frac{\partial u_3}{\partial y} && \text{at } y = h, \\
u_2 &= u_3 && \text{at } y = h, \\
\frac{\partial u_3}{\partial y} &= -\frac{\alpha}{\sqrt{K_3}}(u_3' - Q_2) && \text{at } y = 2h, \\
u_3' &= u_3 && \text{at } y = 2h.
\end{aligned}
$$

(2.7)

Where u_1, u_2 and u_3 are velocities in Regions-I, II and III respectively, K_2 is permeability of the porous medium and K_1, K_3 are permeabilities of lower and upper beds respectively. σ is electrical conductivity of the conducting fluid. B_o is applied magnetic field in the direction normal to the flow. u_1', u_3' are slip velocities at the lower and upper permeable beds respectively and α is the slip parameter. $Q_1 = -\frac{K_1}{\mu_1}\frac{\partial p}{\partial x}$ and $Q_2 = -\frac{K_3}{\mu_3}\frac{\partial p}{\partial x}$ are Darcy's velocities in the upper and lower permeable beds.
In view of pulsating pressure gradient, let us assume that the velocities are in the form

$$u_i = u_{i1} + u_{i2} e^{i\omega t}, \quad i = 1, 2, 3.$$

Where u_{i1} and u_{i2} represent the steady and oscillatory parts of the velocities respectively.

3. Non-dimensionalization of flow quantities

We introduce following non dimensional quantities to make the governing equations and the boundary conditions dimensionless:

$$
\begin{aligned}
x^* &= \frac{x}{h}, y^* = \frac{y}{h}, u_i^* = \frac{u_i}{u}, u_{i1}^* = \frac{u_{i1}}{u}, \\
u_{i2}^* &= \frac{u_{i2}}{u}, t^* = \frac{tu}{h}, K_i^* = \frac{K_i}{h^2}, \\
w^* &= \frac{wh}{u}, p^* = \frac{p}{\rho_1 u^2}, M = B_o h \sqrt{\frac{\sigma}{\mu_2}}.
\end{aligned}
$$

After dropping the asterisks, governing equations of motion $(2.2, 2.4 \& 2.6)$ in non-dimensional form are given by

$$\frac{\partial u_1}{\partial t} = -\frac{\partial p}{\partial x} + \frac{1}{R_1} \frac{\partial^2 u_1}{\partial y^2}.$$

(3.1)

$$\frac{\partial u_2}{\partial t} = -\rho \frac{\partial p}{\partial x} + \frac{1}{R_2} \frac{\partial^2 u_2}{\partial y^2} - \frac{1}{K_2 R_2} u_2 - \frac{M^2}{R_2} u_2.$$

(3.2)

$$\frac{\partial u_3}{\partial t} = -\rho' \frac{\partial p}{\partial x} + \frac{1}{R_3} \frac{\partial^2 u_3}{\partial y^2}.$$

(3.3)

and boundary conditions (2.7) become

$$\frac{\partial u_1}{\partial y} = \alpha\sigma_1\left(u_1' + \frac{R_1}{\sigma_1^2}\frac{\partial p}{\partial x}\right) \quad \text{at } y = -1,$$

$$u_1' = u_1 \qquad\qquad\qquad \text{at } y = -1,$$

$$\beta\frac{\partial u_1}{\partial y} = \frac{\partial u_2}{\partial y} \qquad\qquad \text{at } y = 0,$$

$$u_1 = u_2 \qquad\qquad\qquad \text{at } y = 0,$$

$$\gamma\frac{\partial u_2}{\partial y} = \frac{\partial u_3}{\partial y} \qquad\qquad \text{at } y = 1,$$

$$u_2 = u_3 \qquad\qquad\qquad \text{at } y = 1,$$

$$\frac{\partial u_3}{\partial y} = -\alpha\sigma_2\left(u_3' + \frac{R_3}{\sigma_2^2}\rho'\frac{\partial p}{\partial x}\right) \quad \text{at } y = 2,$$

$$u_3' = u_3 \qquad\qquad\qquad \text{at } y = 2.$$

(3.4)

Where

$$u_i = u_{i1} + u_{i2}e^{i\omega t}, \qquad i = 1, 2, 3$$

$$-\frac{\partial p}{\partial x} = \left(\frac{\partial p}{\partial x}\right)_s + \left(\frac{\partial p}{\partial x}\right)_o e^{i\omega t}$$

are non-dimensional velocities and pressure gradient respectively. $R_1 = \frac{\rho_1 hu}{\mu_1}, R_2 = \frac{\rho_2 hu}{\mu_2}, R_3 = \frac{\rho_3 hu}{\mu_3}$ are Reynolds numbers respectively in flow regions I, II, III, $\sigma_1 = \frac{h}{\sqrt{K_1}}, \sigma_2 = \frac{h}{\sqrt{K_3}}$ are non-dimensional parameters inversely proportional to square root of permeabilities of regions $I\&III$ respectively and $\beta = \frac{\mu_1}{\mu_2}, \gamma = \frac{\mu_2}{\mu_3}, \rho = \frac{\rho_1}{\rho_2}, \rho' = \frac{\rho_1}{\rho_3}$ are non-dimensional parameters. $M = B_o h\sqrt{\frac{\sigma}{\mu_2}}$ is the Hartmann number.

3.1. Steady flow

The governing equations of steady flow are given by

$$\frac{1}{R_1}\frac{d^2 u_{11}}{dy^2} + P_s = 0. \tag{3.5}$$

$$\frac{1}{R_2}\frac{d^2 u_{21}}{dy^2} - \left(\frac{1}{K_2 R_2} + \frac{M^2}{R_2}\right)u_{21} + \rho P_s = 0. \tag{3.6}$$

$$\frac{1}{R_3}\frac{d^2 u_{31}}{dy^2} + \rho' P_s = 0. \tag{3.7}$$

The boundary conditions to be satisfied by u_{i1} are

$$\frac{du_{11}}{dy} = \alpha\sigma_1\left(u_{11}' - \frac{R_1}{\sigma_1^2}P_s\right) \quad \text{at } y = -1,$$

$$u_{11}' = u_{11} \qquad\qquad\qquad \text{at } y = -1,$$

$$\beta\frac{du_{11}}{dy} = \frac{du_{21}}{dy} \qquad\qquad \text{at } y = 0,$$

$$u_{12} = u_{21} \qquad\qquad\qquad \text{at } y = 0,$$

$$\gamma\frac{du_{21}}{dy} = \frac{du_{31}}{dy} \qquad\qquad \text{at } y = 1,$$

$$u_{21} = u_{31} \qquad\qquad\qquad \text{at } y = 1,$$

$$\frac{du_{31}}{dy} = -\alpha\sigma_2\left(u_{31}' - \frac{R_3}{\sigma_2^2}\rho' P_s\right) \quad \text{at } y = 2,$$

$$u_{31}' = u_{31} \qquad\qquad\qquad \text{at } y = 2.$$

(3.8)

Where $P_s = (\frac{\partial p}{\partial x})_s$.

3.2. Oscillatory flow

The governing equations of oscillatory flow are given by

$$\frac{1}{R_1}\frac{d^2 u_{12}}{dy^2} - i\omega u_{12} + P_o = 0. \tag{3.9}$$

$$\frac{1}{R_2}\frac{d^2 u_{22}}{dy^2} - \left(\frac{1}{K_2 R_2} + \frac{M^2}{R_2} + i\omega\right) u_{22} + \rho P_o = 0. \tag{3.10}$$

$$\frac{1}{R_3}\frac{d^2 u_{32}}{dy^2} - i\omega u_{32} + \rho' P_o = 0. \tag{3.11}$$

The boundary conditions to be satisfied by u_{i2} are

$$
\begin{aligned}
\frac{du_{12}}{dy} &= \alpha\sigma_1\left(u'_{12} - \frac{R_1}{\sigma_1^2} P_o\right) & \text{at } y = -1, \\
u'_{12} &= u_{12} & \text{at } y = -1, \\
\beta\frac{du_{12}}{dy} &= \frac{du_{22}}{dy} & \text{at } y = 0, \\
u_{12} &= u_{22} & \text{at } y = 0, \\
\gamma\frac{du_{22}}{dy} &= \frac{du_{32}}{dy} & \text{at } y = 1, \\
u_{22} &= u_{32} & \text{at } y = 1, \\
\frac{du_{32}}{dy} &= -\alpha\sigma_2\left(u'_{32} - \frac{R_3}{\sigma_2^2}\rho' P_o\right) & \text{at } y = 2, \\
u'_{32} &= u_{32} & \text{at } y = 2.
\end{aligned}
\tag{3.12}
$$

Where $P_o = \left(\frac{\partial p}{\partial x}\right)_o$.

4. Solution of the problem

4.1. Steady flow solution

The solution of steady flow described in Section 3.1 is given by

$$u_{11} = C_1 + C_2 y - \frac{1}{2} y^2 P_s R_1. \tag{4.1}$$

$$u_{21} = C_3 \cosh\sqrt{A}y + C_4 \sinh\sqrt{A}y + \frac{\rho P_s R_2}{A}. \tag{4.2}$$

$$u_{31} = C_5 + C_6 y - \frac{1}{2} y^2 \rho' P_s R_3. \tag{4.3}$$

Where $A = M^2 + \frac{1}{K_2}$ and $C_i, i = 1, 2, 3, 4, 5, 6$ are not reported for brevity.

4.2. Oscillatory flow solution

The solution of oscillatory flow described in Section 3.2 is given by

$$u_{12} = C_7 \cosh\sqrt{i\omega R_1}y + C_8 \sinh\sqrt{i\omega R_1}y - \frac{iP_o}{\omega}. \tag{4.4}$$

$$u_{22} = C_9 \cosh\sqrt{B}y + C_{10} \sinh\sqrt{B}y + \frac{\rho P_o R_2}{B}. \tag{4.5}$$

$$u_{32} = C_{11} \cosh\sqrt{i\omega R_3}y + C_{12} \sinh\sqrt{i\omega R_3}y - \frac{i\rho' P_o}{\omega}. \tag{4.6}$$

Where $B = M^2 + \frac{1}{K_2} + i\omega R_2$ and $C_i, i = 7, 8, 9, 10, 11, 12$ are not reported for brevity.

4.3. Pulsatile flow solution

The solution of the pulsatile flow is given by

$$u_1 = u_{11} + u_{12}e^{i\omega t}.$$
$$u_2 = u_{21} + u_{22}e^{i\omega t}.$$
$$u_3 = u_{31} + u_{32}e^{i\omega t}.$$

where u_{11}, u_{21}, u_{31} and u_{12}, u_{22}, u_{32} are known from the steady flow and oscillatory flow solutions given in Eqs. $(4.1), (4.2), (4.3), (4.4), (4.5)$ and (4.6) respectively.

4.4. Mass flux

The instantaneous mass fluxes in Regions I, II and III are respectively given as

$$Q_1 = \int_{-1}^{0} u_{11}dy + \left[\int_{-1}^{0} u_{12}dy\right] e^{i\omega t}.$$

$$Q_2 = \int_{0}^{1} u_{21}dy + \left[\int_{0}^{1} u_{22}dy\right] e^{i\omega t}.$$

$$Q_3 = \int_{1}^{2} u_{31}dy + \left[\int_{1}^{2} u_{32}dy\right] e^{i\omega t}.$$

The elaborated expressions are not given for brevity.

4.5. Shear stress

The shear stresses in non-dimensional form at the both permeable beds are given by

$$\tau_l = \frac{\partial u_1}{\partial y} \qquad \text{at } y = 0.$$

$$\tau_u = \frac{\partial u_3}{\partial y} \qquad \text{at } y = 2.$$

Where τ_l and τ_u are shear stress at the lower and upper permeable beds respectively.

5. Results and discussions

The analytical solutions for the velocity profile of MHD pulsatile flow of conducting fluid in porous medium sandwiched between viscous fluids inside permeable beds are obtained. The analytical solutions are evaluated numerically and depicted graphically in Figs.5.1-5.6, for different values of governing parameters to elucidate interesting features of velocity. In numerical work, we take $\rho = 1, \rho' = 1$ (i.e. $\rho_1 = \rho_2 = \rho_3), R_1 = 2, R_2 = \beta R_1, R_3 = \beta \gamma R_1, \beta = 1.1, \gamma = 1.2, P_s = 2, P_o = 2.5, \alpha = 0.5, K_2 = 3, \sigma_1 = 0.5, \sigma_2 = 0.5$, except where they are variable.

The effect of various flow parameters entering in to problem on pulsating velocity are depicted in Figs. 5.1-5.6. Figs. 5.1(a) and 5.1(b) show the pulsatile velocity profile with respect to y and t simultaneously. It is noticed as Hartmann number M increases, flatness in velocity profile in Regions-I&III increases while in Region-II flatness in velocity profile decreases. Fig. 5.2 shows the variation of pulsating velocity in Region-I (Fig. 5.2(a)), Region-II (Fig. 5.2(b)) and Region-III (Fig. 5.2(c)). The velocities correspond to slip velocities at the interfaces of lower permeable bed ($y = -1$) and upper permeable bed ($y = 2$).

Velocity profiles for permeability of porous medium(K_2), Hartmann number(M), frequency parameter(ωt) and slip parameter(α) are depicted in Fig. 5.3. In Fig. 5.3(a), we see that as K_2 is increasing, the velocity is increasing. From Figs. 5.3(b)& 5.3(c), it is noticed that as M is increasing, the velocity is decreasing. Also we observed that as ωt is increasing, the velocity is increasing(Fig.5.3(d)). For $\sigma_1 = \sigma_2 = 0.5$(Fig. 5.3(e)), as α is increasing, velocity is increasing while For $\sigma_1 = \sigma_2 = 5$(Fig. 5.3(f)), as α is increasing, velocity is decreasing. Fig. 5.4 shows variations of velocity profiles for viscosity ratios β(Fig.5.4(a)) and γ(Fig.5.4(b)). As β and γ are decreasing, the velocity is decreasing. This is due to fact that as the viscosity ratios decrease, the fluids become thicker. Therefore the flow velocity is reduced. Fig. 5.5 illustrates the influence of the porosity parameters $\sigma_1 \& \sigma_2$ on the flow velocity. In Figs. 5.5(a) and 5.5(b), we see that as the porosity parameters increase, the flow velocity decrease.

Finally velocity profiles for some special cases are depicted in Fig. 5.6. Fig. 5.6(a) shows the velocity profile for high Reynolds number R_1(=250) when permeability of porous medium $K_2 \to \infty$. Velocity profile For same fluids($\beta = 1, \gamma = 1, M = 0$) in all regions is shown in Fig. 5.6(b). Further we see that, for same fluids and $K_2 \to \infty$, velocity profile is parabolic (similar to plane Poiseuille flow in a permeable channel)(Fig.5.6(c)). In addition, if porosity parameters $\sigma_1 \to \infty \& \sigma_2 \to \infty$ then permeable beds behave like impermeable plates (Fig.5.6(d)) and the no slip condition follows.

The variation in shear stress τ at the interfaces of lower permeable bed(LPB) and upper permeable bed(UPB) with respect to various flow parameters entering into the problem is presented numerically through Tables 1-6. In Table 1, we have presented the shear stress as R_1 increases for a fixed set of other values of parameters. As R_1 is increasing, the shear stress at both plates is increasing. In Table 2, we notice
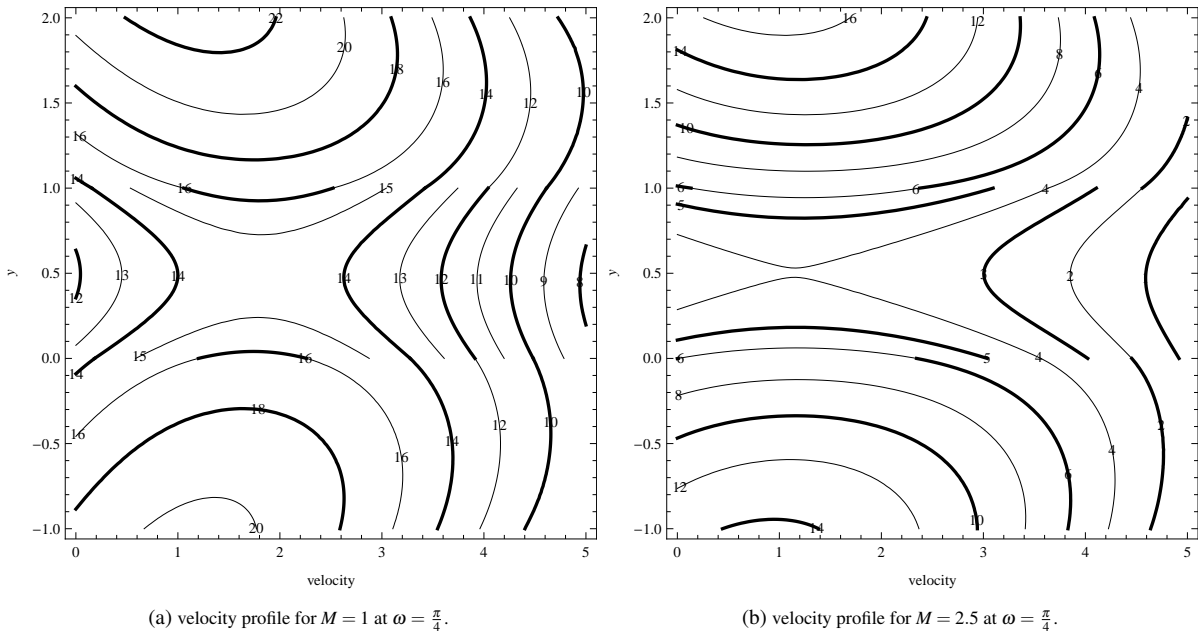
(a) velocity profile for $M = 1$ at $\omega = \frac{\pi}{4}$.

(b) velocity profile for $M = 2.5$ at $\omega = \frac{\pi}{4}$.

Figure 5.1: Velocity profiles for simultaneous variations in y and t

(a) velocity profile in Region-I for y at $M = 0.5, \omega = \frac{\pi}{4}$.

(b) velocity profile in Region-II for y at $M = 0.5, \omega = \frac{\pi}{4}$.

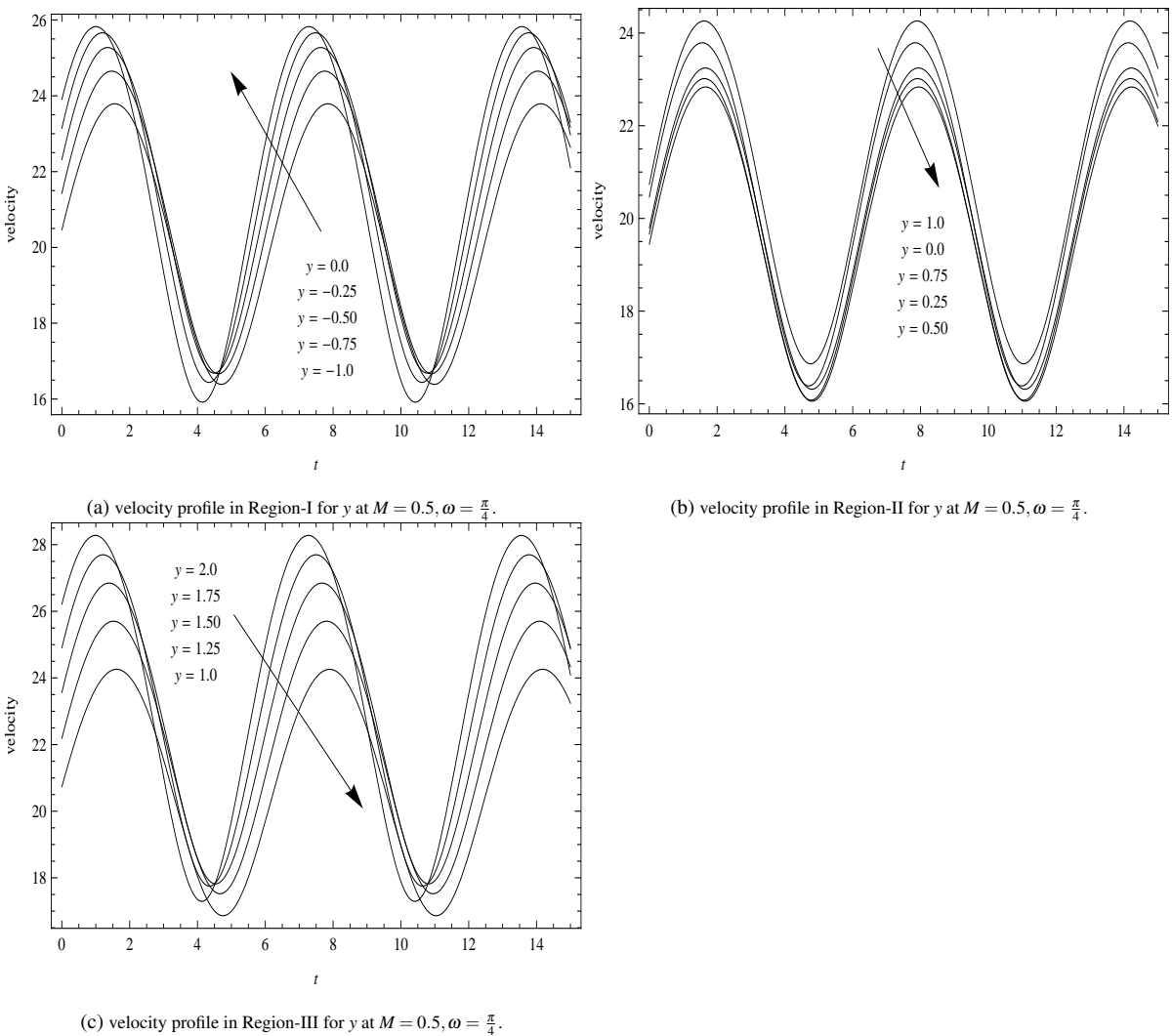(c) velocity profile in Region-III for y at $M = 0.5, \omega = \frac{\pi}{4}$.
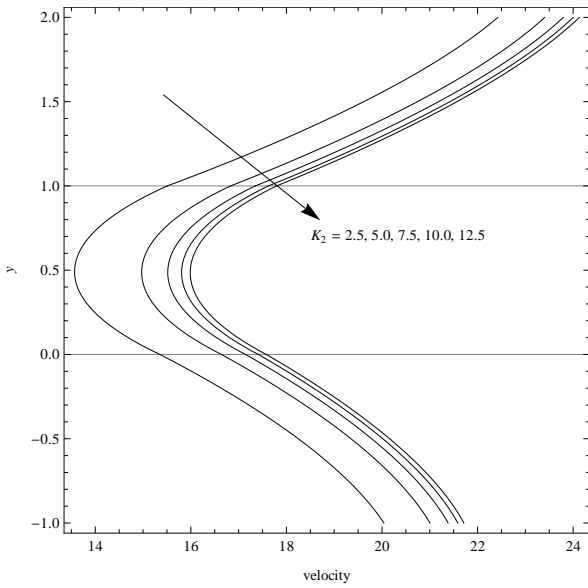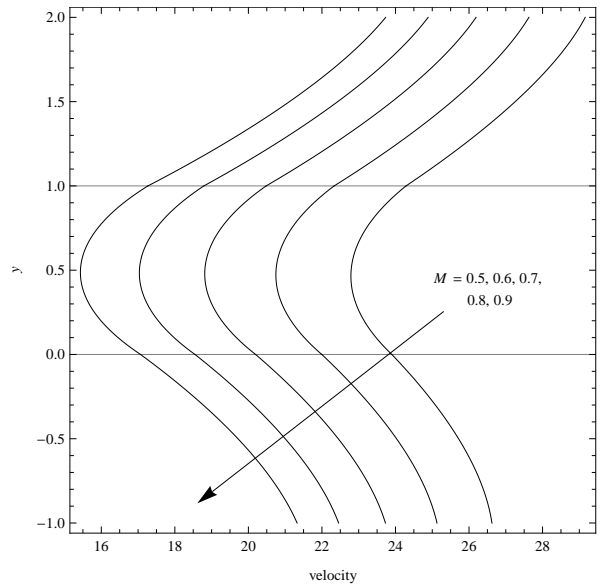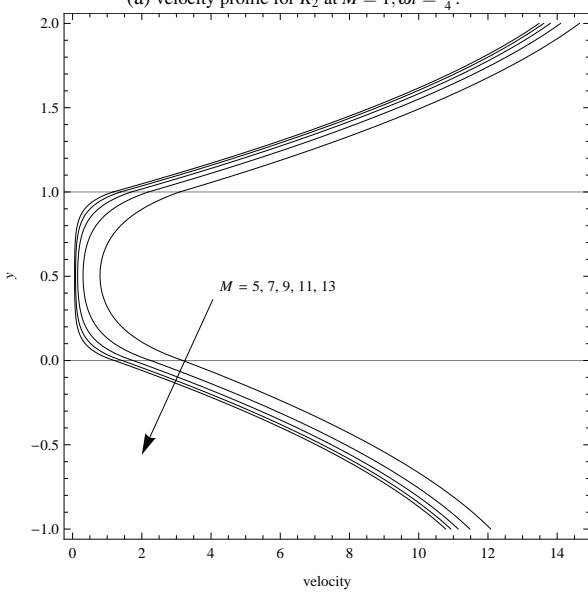
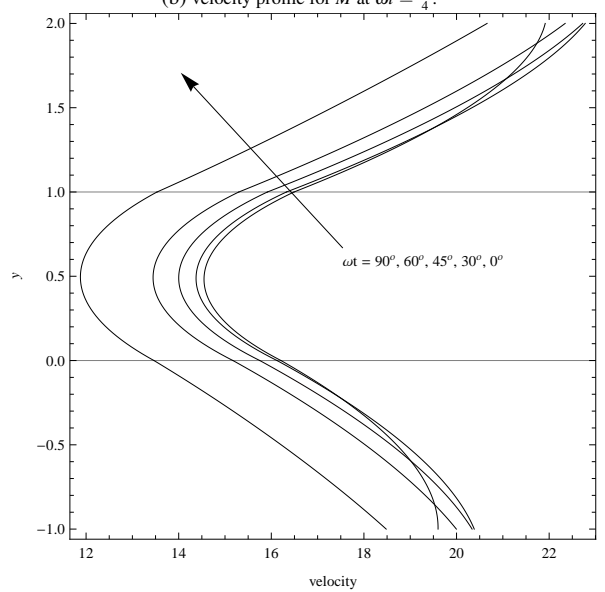**Figure 5.2:** Velocity profiles with time

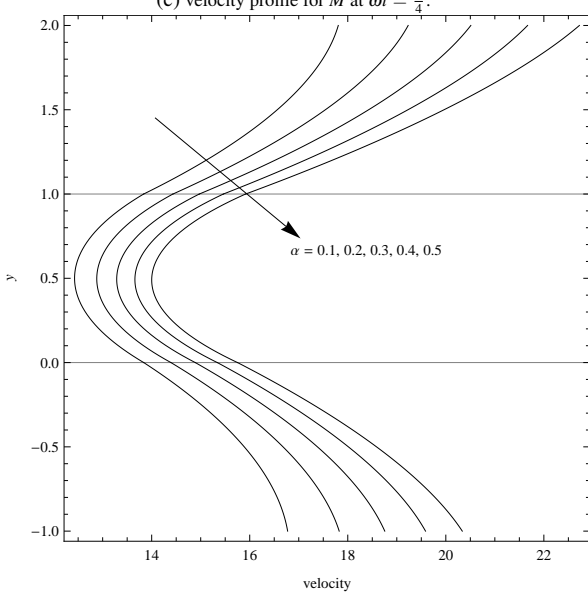(a) velocity profile for K_2 at $M = 1, \omega t = \frac{\pi}{4}$.

(b) velocity profile for M at $\omega t = \frac{\pi}{4}$.

(c) velocity profile for M at $\omega t = \frac{\pi}{4}$.

(d) velocity profile for ωt at $M = 1$.

(e) velocity profile for α at $M = 1$,
$\omega t = \frac{\pi}{4}, \sigma_1 = \sigma_2 = 0.5$.
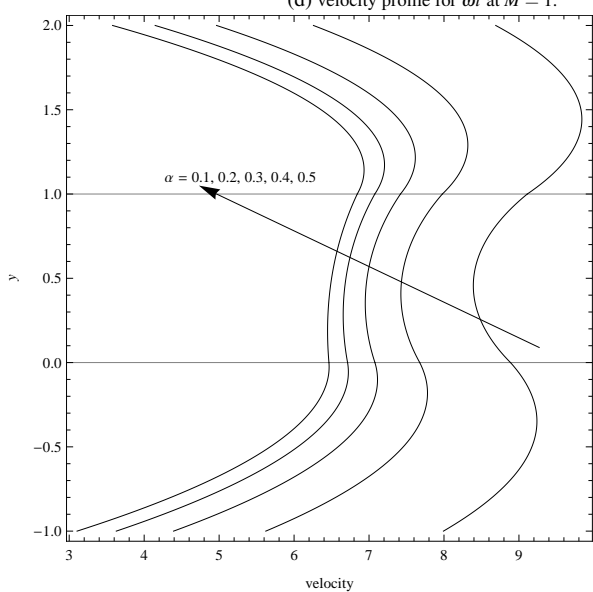
(f) velocity profile for α at $M = 1$,
$\omega t = \frac{\pi}{4}, \sigma_1 = \sigma_2 = 5$.

Figure 5.3: Velocity profiles for permeability(K_2), Hartmann number(M), frequency parameter(ωt), slip parameter(α).

(a) velocity profile for β at $M = 1, \omega t = \frac{\pi}{4}$.

(b) velocity profile for γ at $M = 1, \omega t = \frac{\pi}{4}$.

Figure 5.4: Velocity profiles for viscosity ratios.

(a) velocity profile for σ_1 at $M = 3, \omega t = \frac{\pi}{4}$.

(b) velocity profile for σ_2 at $M = 3, \omega t = \frac{\pi}{4}$.
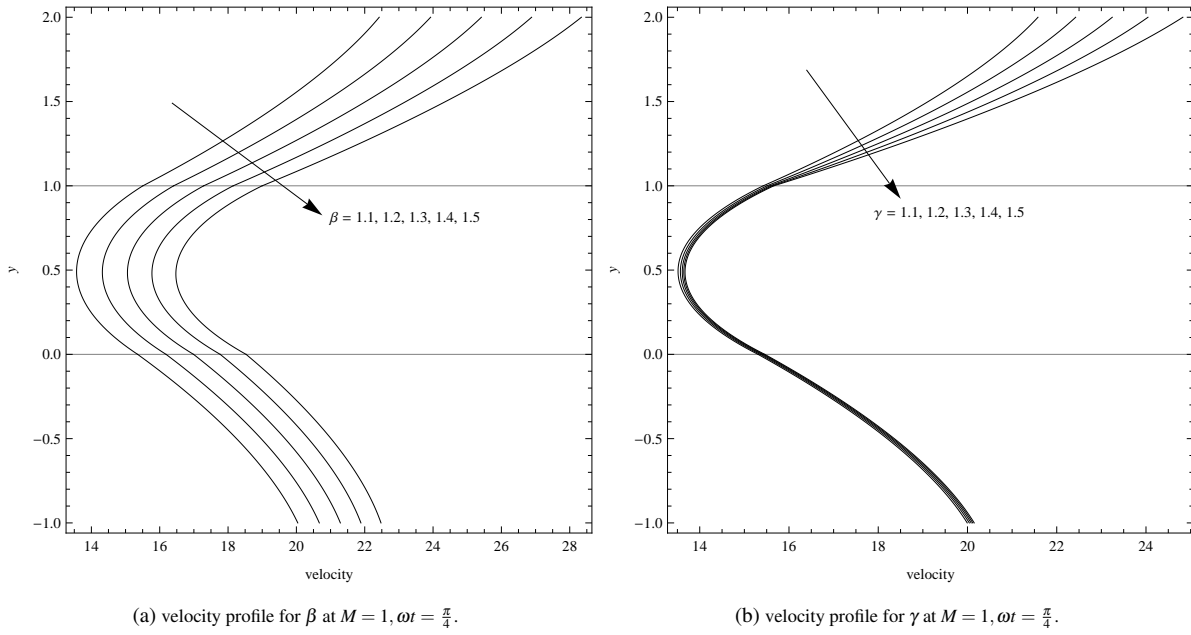
(c) velocity profiles for σ_1, σ_2 at $M = 3, \omega t = \frac{\pi}{4}$.
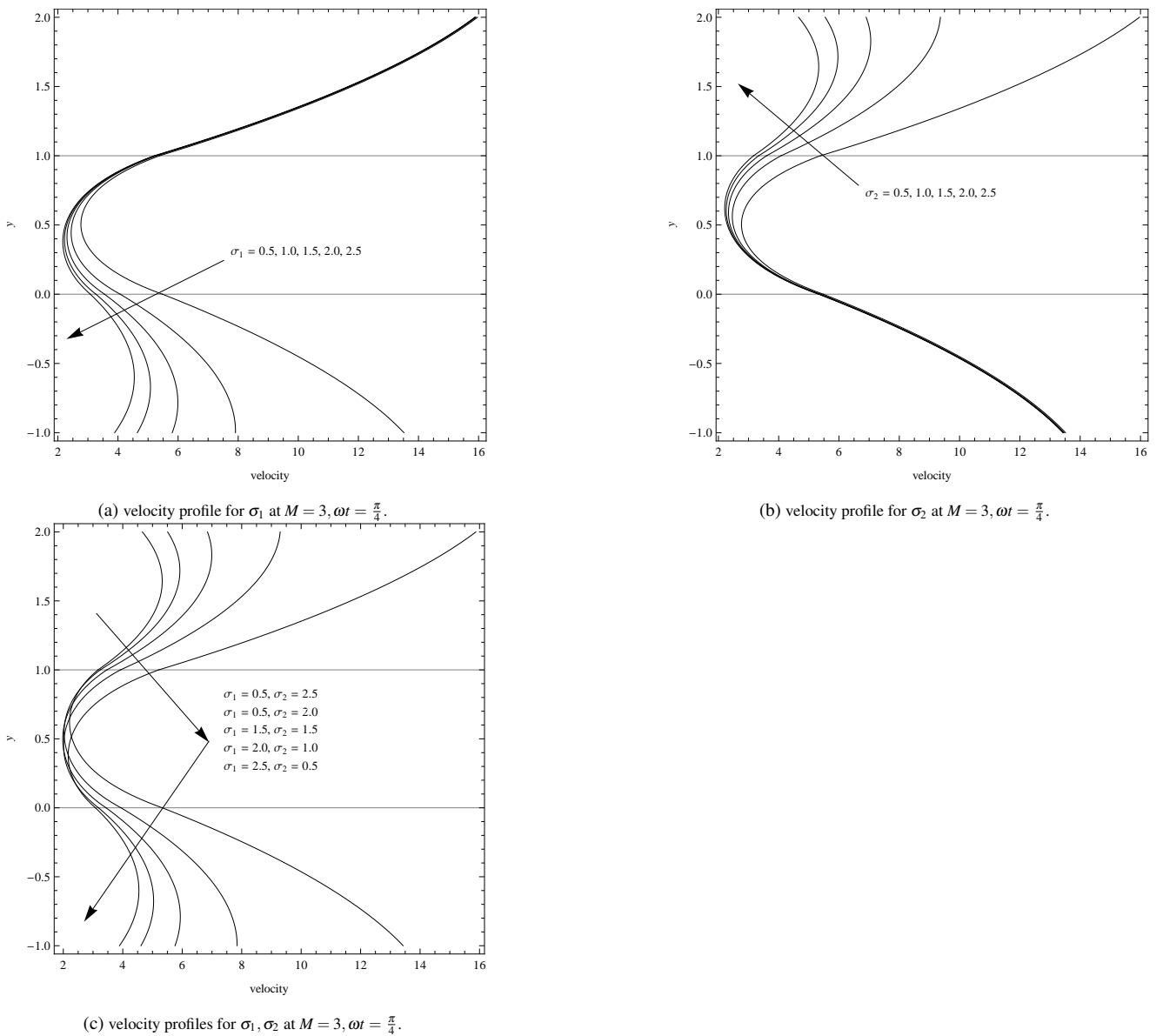
Figure 5.5: Velocity profiles for porosity parameters.
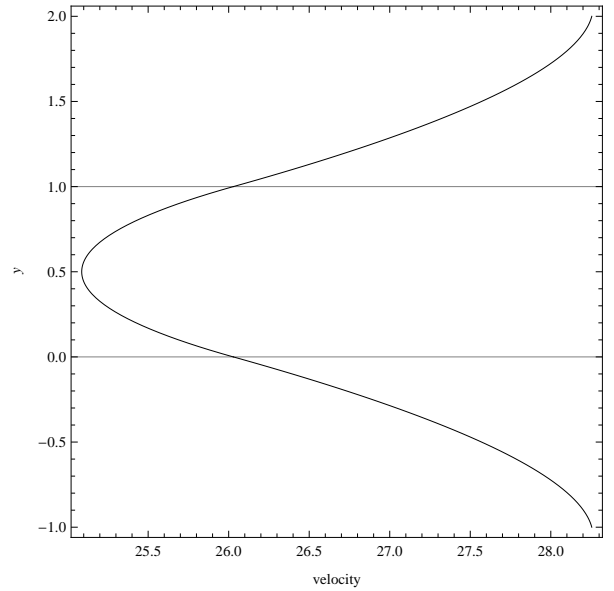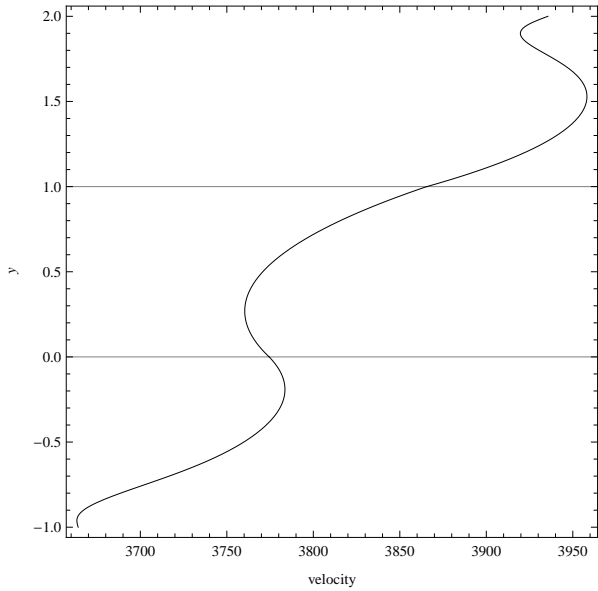
(a) velocity profile for $R_1 = 250$ at $M = 0.5, K_2 \rightarrow \infty, \omega t = \frac{\pi}{4}$.

(b) velocity profile at $M = 0, \omega t = \frac{\pi}{4}$.
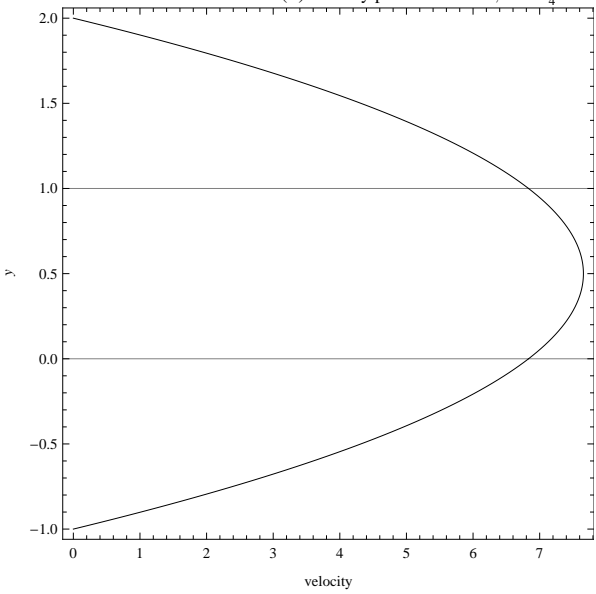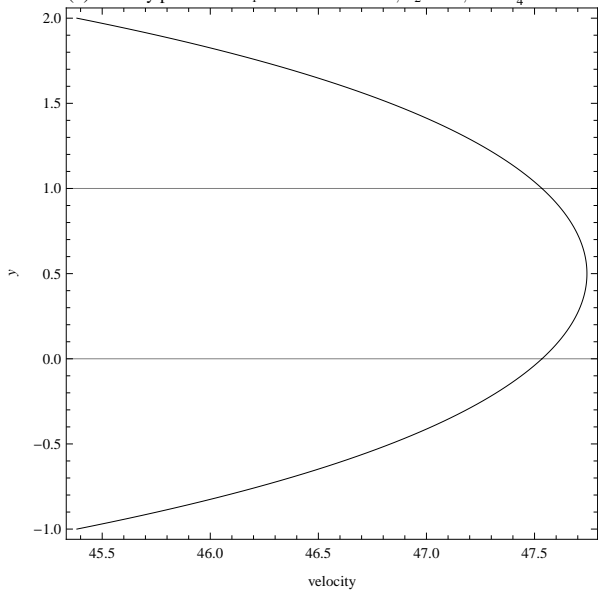
(c) velocity profile at $K_2 \rightarrow \infty, M = 0, \omega t = \frac{\pi}{4}$.

(d) velocity profile at $K_2 \rightarrow \infty, \sigma_1 \rightarrow \infty, \sigma_2 \rightarrow \infty, M = 0, \omega t = \frac{\pi}{4}$.

Figure 5.6: Some special cases.

that as the Hartmann number M in increasing for $\omega t = 0, \frac{\pi}{4}, \frac{\pi}{2}$, shear stress is increasing at both plates. While at $\omega t = \frac{3\pi}{4}$, as M is increasing through values 0 to 1, shear stress is decreasing at both the permeable beds and further an increase in M results an increase in shear stress. In Table 3, it is seen that as the porosity parameter $\sigma(=\sigma_1 = \sigma_2)$ is increasing shear stress is increasing at both the permeable beds. At fixed value of σ, greater or equal to 1.5 as ωt is increasing through values 0 to $\frac{\pi}{4}$, shear stress at both the permeable plates is increasing. Further an increase in ωt results a decrease in shear stress at both permeable beds. Table 4 shows that as slip parameter α is increasing, shear stress is increasing at the both permeable beds.

In Table 5, it is seen that as the viscosity ratio β is increasing for $\omega t = 0, \frac{\pi}{4}$ and $\frac{\pi}{2}$, shear stress at lower permeable bed is decreasing while at upper permeable bed is increasing. However, for $\omega t = \frac{3\pi}{4}$ shear stress at both the permeable beds is increasing. Table 6 shows that as viscosity ratio γ is increasing, shear stress at both the permeable beds is increasing.

Table 1: Variation in shear stress at $\rho = 1, \rho' = 1, \beta = 1.1, \gamma = 1.2, \alpha = 0.1, K_2 = 0.5, M = 0.5, \sigma = 0.5, P_s = 2, P_o = 2.5$.

	$mod\tau$	$R_1 = 1$	$R_1 = 2$	$R_1 = 3$	$R_1 = 4$	$R_1 = 5$
$\omega t = 0$	LPB	0.576235	1.26637	1.94451	2.61591	3.28401
	UPB	0.835937	1.79615	2.73995	3.67603	4.60869
$\omega t = \frac{\pi}{4}$	LPB	0.511393	1.15577	1.79376	2.42633	3.05605
	UPB	0.74404	1.63640	2.51935	3.39597	4.26958
$\omega t = \frac{\pi}{2}$	LPB	0.394241	0.930285	1.46393	1.99331	2.52031
	UPB	0.563685	1.28775	2.00798	2.72324	3.43396
$\omega t = \frac{3\pi}{4}$	LPB	0.275511	0.684203	1.08954	1.49088	1.89003
	UPB	0.359703	0.874562	1.38495	1.89074	2.39423

Table 2: Variation in shear stress at $\rho = 1, \rho' = 1, \beta = 1.1, \gamma = 1.2, \alpha = 0.1, K_2 = 0.5, R_1 = 0.5, \sigma = 0.5, P_s = 2, P_o = 2.5$.

	$mod\tau$	$M = 0$	$M = 1$	$M = 2$	$M = 3$	$M = 4$
$\omega t = 0$	LPB	0.234249	0.261655	0.302353	0.326433	0.339460
	UPB	0.357861	0.385929	0.425848	0.449225	0.461851
$\omega t = \frac{\pi}{4}$	LPB	0.201686	0.227863	0.270706	0.295819	0.309167
	UPB	0.311327	0.339955	0.382696	0.407355	0.420455
$\omega t = \frac{\pi}{2}$	LPB	0.147856	0.163184	0.199394	0.221357	0.232903
	UPB	0.225843	0.246331	0.283357	0.305139	0.316599
$\omega t = \frac{3\pi}{4}$	LPB	0.097197	0.0860313	0.102392	0.116566	0.124215
	UPB	0.131169	0.128155	0.147005	0.161133	0.168830

Table 3: Variation in shear stress at $\rho = 1, \rho' = 1, \beta = 1.1, \gamma = 1.2, \alpha = 0.1, K_2 = 0.5, M = 0.5, R_1 = 0.5, P_s = 2, P_o = 2.5$.

	$mod\tau$	$\sigma = 0.5$	$\sigma = 1.5$	$\sigma = 2.5$	$\sigma = 3.5$	$\sigma = 4.5$
$\omega t = 0$	LPB	0.242167	0.379546	0.658378	0.857072	1.01040
	UPB	0.366173	0.384147	0.706753	0.938218	1.11837
$\omega t = \frac{\pi}{4}$	LPB	0.20864	0.406545	0.680018	0.873209	1.02041
	UPB	0.319456	0.419315	0.736508	0.962566	1.13679
$\omega t = \frac{\pi}{2}$	LPB	0.150494	0.371778	0.598397	0.756888	0.876073
	UPB	0.230816	0.390812	0.654390	0.840841	0.982867
$\omega t = \frac{3\pi}{4}$	LPB	0.090721	0.280585	0.426084	0.526122	0.599565
	UPB	0.127775	0.303020	0.473024	0.59185	0.680481

Table 4: Variation in shear stress at $\rho = 1, \rho' = 1, \beta = 1.1, \gamma = 1.2, R_1 = 0.5, K_2 = 0.5, M = 0.5, \sigma = 0.5, P_s = 2, P_o = 2.5$.

	$mod\,\tau$	$\alpha = 0.1$	$\alpha = 0.2$	$\alpha = 0.3$	$\alpha = 0.4$	$\alpha = 0.5$
$\omega t = 0$	LPB	0.242167	0.446143	0.619790	0.769034	0.898413
	UPB	0.366173	0.682074	0.956955	1.19801	1.41084
$\omega t = \frac{\pi}{4}$	LPB	0.208640	0.382286	0.528574	0.653148	0.760256
	UPB	0.319456	0.591913	0.826586	1.03050	1.20911
$\omega t = \frac{\pi}{2}$	LPB	0.150494	0.27481	0.378936	0.467211	0.542847
	UPB	0.230816	0.425289	0.590973	0.733524	0.857272
$\omega t = \frac{3\pi}{4}$	LPB	0.0907217	0.168961	0.237268	0.29748	0.35097
	UPB	0.127755	0.236725	0.330798	0.41289	0.485178

Table 5: Variation in shear stress at $\rho = 1, \rho' = 1, \gamma = 1.2, \alpha = 0.1, R_1 = 0.5 K_2 = 0.5, M = 0.5, \sigma = 0.5, P_s = 2, P_o = 2.5$.

	$mod\,\tau$	$\beta = 1.1$	$\beta = 1.2$	$\beta = 1.3$	$\beta = 1.4$	$\beta = 1.5$
$\omega t = 0$	LPB	0.242167	0.235693	0.229787	0.224480	0.219647
	UPB	0.366173	0.406497	0.447604	0.489375	0.531704
$\omega t = \frac{\pi}{4}$	LPB	0.208640	0.202891	0.198229	0.194543	0.191758
	UPB	0.319456	0.355058	0.391547	0.428814	0.466753
$\omega t = \frac{\pi}{2}$	LPB	0.150494	0.148264	0.147592	0.148340	0.150339
	UPB	0.230816	0.257663	0.285451	0.314073	0.343430
$\omega t = \frac{3\pi}{4}$	LPB	0.090721	0.095987	0.102598	0.110203	0.118511
	UPB	0.127775	0.14550	0.164142	0.18358	0.203701

Table 6: Variation in shear stress at $\rho = 1, \rho' = 1, \beta = 1.1, \alpha = 0.1, R_1 = 0.5, K_2 = 0.5, M = 0.5, \sigma = 0.5, P_s = 2, P_o = 2.5$.

	$mod\,\tau$	$\gamma = 1.1$	$\gamma = 1.2$	$\gamma = 1.3$	$\gamma = 1.4$	$\gamma = 1.5$
$\omega t = 0$	LPB	0.242042	0.242167	0.242297	0.242431	0.242566
	UPB	0.323116	0.366173	0.409472	0.452474	0.496653
$\omega t = \frac{\pi}{4}$	LPB	0.208492	0.20864	0.208794	0.208952	0.209112
	UPB	0.280799	0.319456	0.358420	0.397632	0.437051
$\omega t = \frac{\pi}{2}$	LPB	0.150302	0.150494	0.150686	0.150879	0.151071
	UPB	0.202437	0.230816	0.259588	0.288665	0.317987
$\omega t = \frac{3\pi}{4}$	LPB	0.090445	0.090721	0.090984	0.091235	0.091475
	UPB	0.113949	0.127775	0.142160	0.156977	0.172135

6. CONCLUSION

The problem of MHD pulsatile fluid of viscous conducting flow in porous medium sandwiched between viscous fluids is analysed inside permeable beds of different permeability. Separate expressions for velocity and mass flux in both regions are obtained using B-J slip boundary condition at the interfaces of permeable beds. The analytical solutions are evaluated numerically and depicted graphically to elucidate the features of velocity and shear stress for various values of Hartmann number M, Reynolds number R_1, permeability of porous medium K_2, frequency parameter ωt, slip parameter α, viscosity ratios β and γ and non-dimensional parameters σ_1, σ_2. It is observed that Hartmann number M and non-dimensional parameters σ_1, σ_2 suppress the flow velocity while permeability of porous medium K_2, frequency parameter ωt and viscosity ratios β and γ promote the flow. Variation of pulsatile velocity with slip parameter α depends on σ_1, σ_2. For $\sigma_1 = \sigma_2 = 0.5$, α promotes the flow while for $\sigma_1 = \sigma_2 = 5$, α supress the flow. As the slip parameter, Reynolds number and viscosity ratio γ are increasing, shear stress at both the permeable beds are increasing. Shear stress shows mix trends with Hartmann number, porosity parameters and viscosity ratio β.

References

[1] Beavers, G. and D. Joseph, Boundary conditions at naturally permeable wall, J. Fluid Mech Vol:30,No.1(1967), 197-207.

[2] Bhattacharyya, P., Unsteady laminar flow in a channel with porous bed, J.Indian Inst. Sci Vol:62(B)(1980), 89-99.

[3] Carpinlioglu, M. O., An overview on pulsatile flow dynamics, Journal of Thermal Engineering,Vol:1,No.3(2015), 496-504.

[4] D.A.Nield, Modelling fluid flow and heat transfer in a saturated porous medium, Journal of applied mathematics and decision sciences Vol:4,No.2(2000), 165-173.

[5] Iyengar, T.K.V. and P. Bitla, Pulsating flow of an incompressible couple stress fluid between permeable beds. International Journal of Mathematical, Computational, Physical, Electrical and Computer Engineering Vol:5,No.8(2011), 1241-1251.

[6] Jogie, D. and B. Bhatt, Flow of immiscible fluids in a naturally permeable channel, International Journal of Pure and Applied Mathematics Vol:78,No.3(2012), 435-449.

[7] Khan, A. and G. Zaman, Unsteady magnetohydrodynamic flow of second grade fluid due to uniform accelerating plate, Journal of Applied Fluid Mechanics Vol:9,No.6(2016), 3127-3133.

[8] Ku, D., D. Giddens, C. Zairns, and S. Glagov, Pulsatile flow and atherosclerosis in human carotid bifurcation, Arterioscler Thromb. Vasc. Biol. Vol:5,No.3(1985), 293-302.

[9] Panda, S., S. C. Martha, and A. Chakrabarti, Three layer fluid flow over a small obstruction on the bottom of a channel, The Anziam journal Vol:56,No.3(2015), 248-274.

[10] Prasad, B. and A. Kumar, Flow of a hydromagnetic fluid through porous media between permeable beds under exponentially decaying pressure gradient, Computational methods in science and technology Vol:17,No.1(2011), 63-74.

[11] Shit, G. C. and M. Roy, Hydromagnetic pulsating flow of blood in a constricted porous channel: A theoretical study, In Proceedings of the World Congress on Engineering, London, U.K. Vol:1(2012).

[12] Siddiqui, A. M., N. Z. Khan, M. A. Rana, and T. Haroon, Flow of a second grade fluid through constricted tube using integral method, Journal of Applied Fluid Mechanics Vol:9,No.6(2016), 2803-2812.

[13] Sreenadh, S., A. Parandhama, and R. Hemadrireddy, Unsteady flow of couple stress fluid in contact with a newtonian fluid between permeable beds, International J. of Math. Sci. and Engg. Appls. (IJMSEA) Vol:6,No.IV(2012), 241–258.

[14] Srinivas, J. and J. V. R. Murthy, Flow of two immiscible couple stress fluids between two permeable beds Journal of Applied Fluid Mechanics Vol:9,No.1(2016), 501-507.

[15] Sulochana, P., Unsteady MHD pulsatile flow of couple stress fluid under the influence of periodic body acceleration between two parallel plates, Advances in Applied Science Research Vol:5,No.4(2014), 136-143.

[16] Umavathi, J., A. J. Chamakha, A. Mateem, and A. Al-Mudhaf, Unsteady oscillatory flow and heat transfer in a horizontal composite porous medium channel, Non-linear Analysis:Modelling and Control Vol:14,No.3(2009), 397-415.

[17] Umavathi, J. C., I. Leu, J. P. Kumar, and D. S. Meera, Unsteady flow and heat transfer of porous media sandwiched between viscous fluids, Appl. Math. and Mech. - Engl. Ed. Vol;31,No.12(2010), 1497-1516.

[18] Venugopal, R. and D. Bathaiah, Magnetohydrodynamic flow past a permeable bed, Def Sci J. Vol:33,No.1(1983), 69-90.

[19] Yamamoto, K. and Z. Yoshida, Flow through a porous wall with convective acceleration, Journal of Physical Society of Japan Vol.37,No.3 (1974), 774-779.

[20] Zamir, M.,*The Physics of Pulsatile Flow, Springer-Verlag, (2000).*